

## Electronic Supplementary Material

# CO<sub>2</sub>-promoted hydrogen production in a protonic ceramic electrolysis cell

Nikolay Danilov,<sup>a,b</sup> Julia Lyagaeva,<sup>a,b</sup> Arthem Tarutin,<sup>a,b</sup>  
Gennady Vdovin,<sup>a</sup> Dmitry Medvedev<sup>\*a,b</sup>

<sup>a</sup> Laboratory of Electrochemical Devices Based on Solid Oxide Proton Electrolytes, Institute of High Temperature Electrochemistry, Yekaterinburg 620137, Russia

<sup>b</sup> Ural Federal University, Yekaterinburg 620002, Russia

\*E-mail: dmitrymedv@mail.ru

## Experimental

### Materials synthesis

The  $\text{BaCe}_{0.3}\text{Zr}_{0.5}\text{Dy}_{0.2}\text{O}_{3-\delta}$  (BCZDy) powder material was prepared by a citrate-nitrate combustion route, using  $\text{Ba}(\text{NO}_3)_2$ ,  $\text{Ce}(\text{NO}_3)_3 \cdot 6\text{H}_2\text{O}$ ,  $\text{Dy}(\text{NO}_3)_3 \cdot 5\text{H}_2\text{O}$ ,  $\text{ZrO}(\text{NO}_3)_2$  as initial components with purity not less than 99.5%. They were taken in the strictly required amounts and dissolved in distilled water until complete salts dissolution. The obtained solution was heated at 80 °C and then citric acid was added in a mole amount exceeding by 2 times a total metal cations amount. A pH value of the solution around 7.0 was regulated by adding ammonia water. The resulting solution was heat-treated at 250 °C until self-ignition and producing a high disperse brown powder. The latter was calcined at 700 °C (1 h) to remove organic substances, pre-synthesized at 1050 °C (5 h) to reach material crystallization and synthesized at 1150 °C (5 h) to obtain the single-phase product; each temperature treatment was accompanied by powder milling. To ensure good densification behavior of the electrolyte and to suppress the refractory nature of  $\text{Zr}^{4+}$ , a sintering additive of CuO was added in a small amount (0.5 wt%) after citric acid dissolution.

The  $\text{Nd}_{1.95}\text{Ba}_{0.05}\text{NiO}_{4+\delta}$  (NBN) powder material was prepared using a similar method, differing only by temperature treatments: 700 °C (1 h), 900 °C (3 h) and 1100 °C (5 h) for calcination, pre-synthesis and synthesis steps, respectively.

### Materials characterization

The synthesized materials were analyzed by the X-ray diffraction (XRD) method. The data were obtained using the Rigaku Co. Ltd. D/MAX-2200 diffractometer [S1] under the following conditions:  $\text{CuK}\alpha$  radiation, within  $20 \leq 2\theta,^\circ \leq 80$  range, with a  $2^\circ \text{min}^{-1}$  scan rate and a  $0.02^\circ$  scan step. The XRD analysis was performed for the individual materials, for the BCZDy/NBN powder mixture to confirm chemical compatibility and BCZDy treated at 700 °C (5 h) by air passed through the boiling water and 100%  $\text{CO}_2$  to check chemical stability in the aggressive media.

The images of morphology of the electrochemical cell's cross-section were obtained using scanning electron microscopy (SEM) method, a microscope TESCAN MIRA 3 LMU [S1].

### The PCEC fabrication and characterisation

The protonic ceramic electrolysis cell (PCEC) was fabricated using a tape calendering method [S2], which is based on the co-rolling of the films consisted of the corresponding (BCZDy, NiO-BCZDy) powders in a special organic binder. Then the co-rolled films were treated at 900 °C (slow heating and cooling) to burn the carbon and organic components and then sintered at 1450 °C (5 h) to form the half-cell. To produce the single PCEC, the NBN-BCZDy slurry (7:3 wt ratio) was painted onto the electrolyte surface of the half-cell and sintered at 1100 °C for 1 h. No electrocatalytic methods (exsolution, infiltration) were used to improve the activity of the oxygen electrode.

The PCEC's performance was analyzed at 700 °C varying gas compositions at the both cathode and anode sides. The air with different water vapor partial pressure values ( $p_{\text{H}_2\text{O}} = 0.01, 0.03,$

0.1, 0.2 and 0.3 atm) was used as an oxidizing atmosphere, while wet hydrogen with different carbon dioxide partial pressure ( $p_{\text{CO}_2} = 0, 0.5, 0.7, 0.8$  and  $0.9$  atm,  $p_{\text{H}_2\text{O}} = 0.03$  atm) was used as a reducing atmosphere. The  $p_{\text{H}_2\text{O}}$  level was regulated by passing the gases through a bubbler heated at a specified temperature to reach desirable saturation. The  $p_{\text{CO}_2}$  level was regulated by mixing the  $\text{H}_2$  and  $\text{CO}_2$  fluxes, taking into account their flow rates. The flow rates of oxidizing and reducing gases were equal to  $30$  and  $100 \text{ ml min}^{-1}$ , respectively.

The electrochemical characterization was performed by means of a potentiostat/galvanostat Amel M2550 (Italy) and a FRA box MaterialsM Instruments (Italy). Volt-ampere curves were recorded within an applied voltage range from open circuit voltage (OCV) to  $1.6 \text{ V}$  and a step of  $0.025 \text{ mV}$ . Impedance spectra were obtained at three bias voltages ( $1.0, 1.3$  and  $1.6 \text{ V}$ ) in a frequency range of  $10^{-1}$ – $10^5 \text{ Hz}$  and amplitude signal of  $15$ – $20 \text{ mV}$ . The impedance data were analyzed by the means of equivalent circuit models (Zview software) and distribution of relaxation times (DRT) method [S3].

## Tables

**Table S1** Comparison of PCECs' performance: h is the thickness, T is the temperature,  $R_t$ ,  $R_o$  and  $R_p$  are the total, ohmic and polarization resistances at open circuit voltage mode ( $i = 0 \text{ A cm}^{-2}$ ) or \*thermoneutral voltage mode (bias is equal  $\sim 1.3 \text{ V}$ ),  $i$  is the current density at  $U = 1.3 \text{ V}$ ,  $i_{\text{eff.}}$ \* is the effective current density of PCECs based on the electrolytes with thickness reduced to  $10 \mu\text{m}$ .

Electrolyte		Anode composition	Gas composition		T, °C	$R_t$ , $\Omega \text{ cm}^2$	$R_o$ , $\Omega \text{ cm}^2$	$R_p$ , $\Omega \text{ cm}^2$	i, $\text{mA cm}^{-2}$	$i_{\text{eff.}}$ , $\text{mA cm}^{-2}$	Ref.
Composition	h, $\mu\text{m}$		Anode	Cathode							
BCZDy	50	NBN–BCZDy (7:3)	30% $\text{H}_2\text{O}/\text{air}$	3% $\text{H}_2\text{O}/\text{H}_2$	700	0.67*	0.50*	0.17*	542	1345	This work
BCZDy	50	NBN–BCZDy (7:3)	30% $\text{H}_2\text{O}/\text{air}$	3% $\text{H}_2\text{O}/(50\text{H}_2+50\text{CO}_2)$	700	0.64*	0.49*	0.15*	628	1620	This work
BCZY0.3	20	SSC–BCZY0.3 (7:3)	30% $\text{H}_2\text{O}/\text{air}$	$\text{H}_2$	700	0.93*	0.52*	0.41*	380	530	[S4]
BCZYZ	75	LSMC–BCZYZ (65:35)	3% $\text{H}_2\text{O}/\text{N}_2$	5% $\text{H}_2/\text{Ar}$	700	0.89*	0.71*	0.18*	993	3200	[S5]
BCZYZ	60	F–BCZYZ (65:35)	3% $\text{H}_2\text{O}/\text{H}_2$	100% $\text{CO}_2$	614	-	-	-	315	-	[S6]
BZY	15	LSCF–BZY	3% $\text{H}_2\text{O}/\text{air}$	4% $\text{H}_2/\text{Ar}$	700	-	-	-	207	-	[S7]
BCZY0.1	15	$\text{La}_{1.2}\text{Sr}_{0.8}\text{NiO}_{4+\delta}$	20% $\text{H}_2\text{O}/\text{air}$	3% $\text{H}_2\text{O}/\text{H}_2$	700	0.49	0.22	0.27	1370	1610	[S8]
BCZY0.1	15	SEFC–BCZY0.1 (95:5)	10% $\text{H}_2\text{O}/\text{air}$	3% $\text{H}_2\text{O}/\text{H}_2$	700	0.45	0.33	0.12	1050	1390	[S9]

Electrolyte abbreviations: BCZDy =  $\text{BaCe}_{0.3}\text{Zr}_{0.5}\text{Dy}_{0.2}\text{O}_{3-\delta}$ , BCZY0.3 =  $\text{BaCe}_{0.5}\text{Zr}_{0.3}\text{Y}_{0.2}\text{O}_{3-\delta}$ , BCZYZ =  $\text{BaCe}_{0.5}\text{Zr}_{0.3}\text{Y}_{0.16}\text{Zn}_{0.04}\text{O}_{3-\delta}$ , BZY =  $\text{BaZr}_{0.8}\text{Y}_{0.2}\text{O}_{3-\delta}$ , BCZY0.1 =  $\text{BaCe}_{0.7}\text{Zr}_{0.1}\text{Y}_{0.2}\text{O}_{3-\delta}$ .

Electrode abbreviations: NBN =  $\text{Nd}_{1.95}\text{Ba}_{0.05}\text{NiO}_{4+\delta}$ , SSC =  $\text{Sm}_{0.5}\text{Sr}_{0.5}\text{CoO}_{3-\delta}$ , LSMC =  $(\text{La}_{0.75}\text{Sr}_{0.25})_{0.95}\text{Mn}_{0.5}\text{Cr}_{0.5}\text{O}_{3-\delta}$ , F =  $\text{Fe}_2\text{O}_3$ , LSCF =  $\text{La}_{0.6}\text{Sr}_{0.4}\text{Co}_{0.2}\text{Fe}_{0.8}\text{O}_{3-\delta}$ , SEFC =  $\text{SrEu}_2\text{Fe}_{1.8}\text{Co}_{0.2}\text{O}_{7+\delta}$ .

\* Since the listed data were obtained for PCECs with different design and materials, their performance can be compared estimating the  $i_{\text{eff.}}$  values for the cells with the same electrolyte thickness. These values were calculated on the base of the following assumptions: (i) the electrolyte thickness is reduced to  $10 \mu\text{m}$ , (ii) current density is inversely proportional to  $R_t$ , (iii)  $R_p$  does not change with varying the electrolyte thickness, and (iv) h and  $R_o$  values are decreased by the same magnitude, which follows from the constant conductivity level of the electrolyte membranes ( $\sigma = h/R_o$ ). The highest  $i_{\text{eff.}}$  for the cell studied in ref. [S5] can be associated with either an overestimated current density or a high error in the assumptions drawn.

**Table S2** Equilibrium concentration of gas components<sup>†</sup> at 700 °C depending on the initial gas mixture composition supplied to the cathode side.

Partial pressures in initial gas mixture, atm			Equilibrium partial pressures, atm			
pH <sub>2</sub> O	pH <sub>2</sub>	pCO <sub>2</sub>	pH <sub>2</sub> O	pH <sub>2</sub>	pCO <sub>2</sub>	pCO
0.03	0.97	-	0.03	0.97	-	-
0.03	0.485	0.485	0.235*	0.280	0.280	0.205
0.03	0.291	0.679	0.205	0.116	0.504	0.175
0.03	0.194	0.776	0.166	0.058	0.640	0.136
0.03	0.097	0.873	0.109	0.018	0.794	0.079

The highest pH<sub>2</sub>O value is marked by \*.

---

<sup>†</sup> The equilibrium partial pressures of components were calculated according to law of mass action for the water gas shift reaction



and its equilibrium constant at 973.15 K.

## Figures

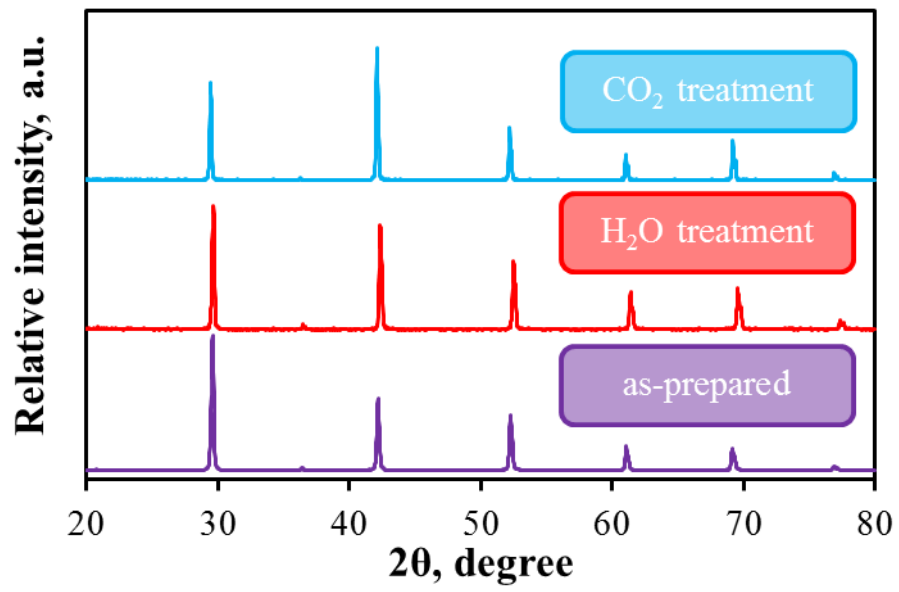


**Fig. S1** XRD patterns for the as-sintered BaCe<sub>0.3</sub>Zr<sub>0.5</sub>Dy<sub>0.2</sub>O<sub>3-6</sub> sample and ones treated by ~100% H<sub>2</sub>O and 100% CO<sub>2</sub> at 700 °C for 5 h.

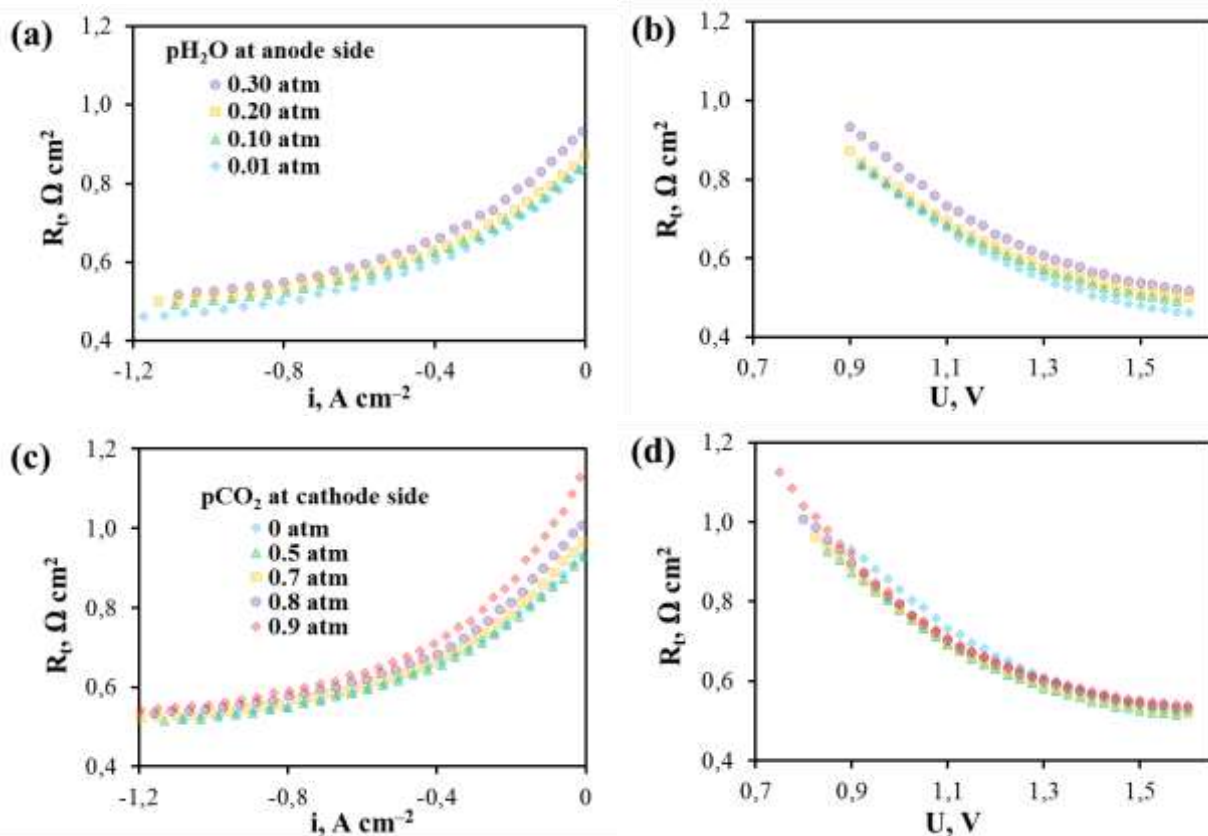


**Fig. S2** Performance of the developed PCEC at 700 °C in term of its total cell resistance ( $R_t$ ) as a function of current density (a,c) or applied voltage (b,d) at different pH<sub>2</sub>O at the anode side (a,b) and pCO<sub>2</sub> at the cathode side (c,d). The  $R_t$  values were calculated on the base of the differential forms of volt-ampere dependences.

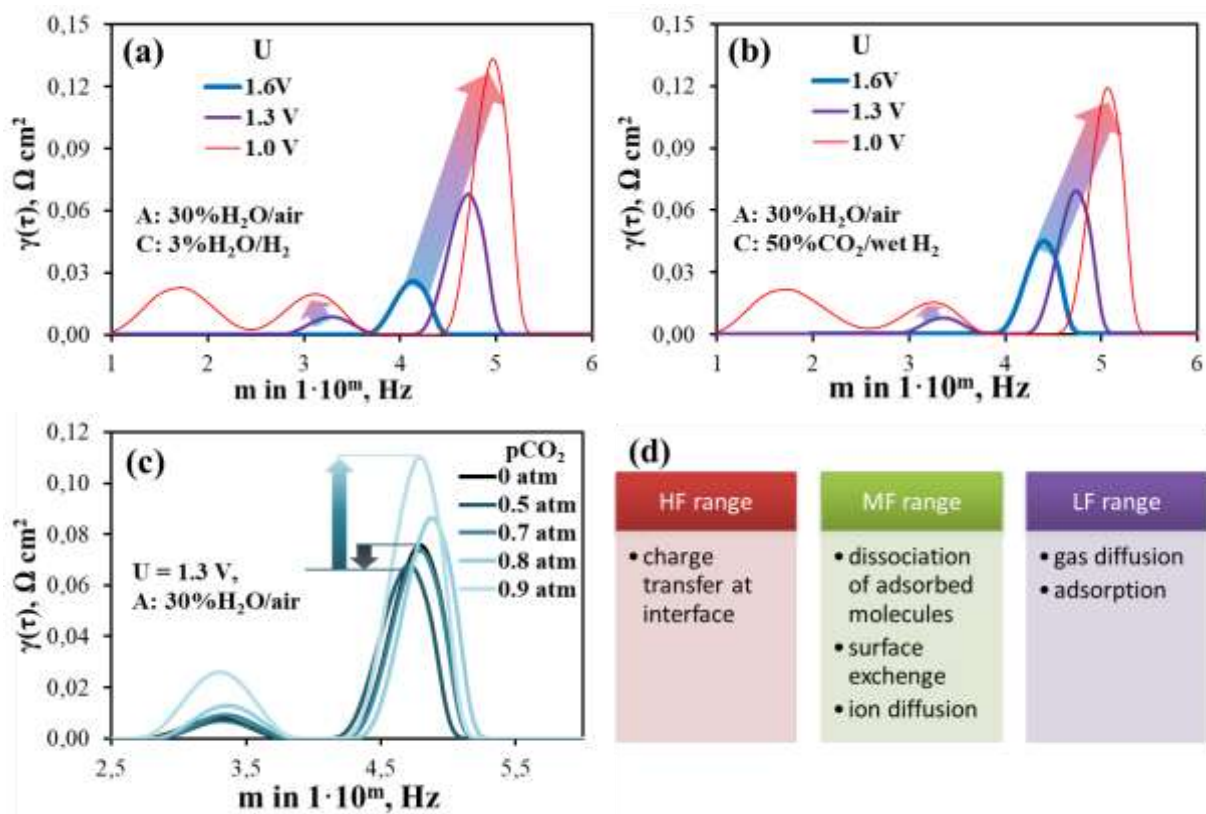


**Fig. S3** DRT analysis of EIS data (a–c). The description is similar with **Fig. 3**; (d) the frequency ranges (high, medium and low) and corresponding electrode processes.<sup>S10–S12</sup>



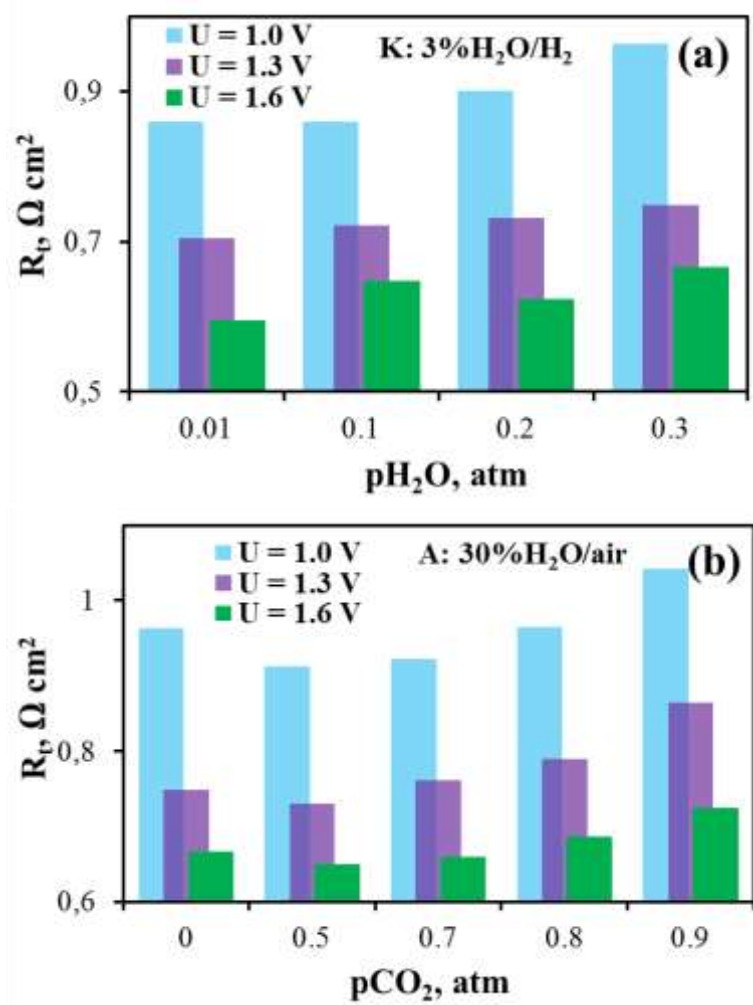


**Fig. S4** Total resistance of the NBN-BCZDy|BCZDy|Ni-BCZDy electrolysis cell at 700 °C and the different bias depending on  $p_{\text{H}_2\text{O}}$  at the anode side (a) and  $p_{\text{CO}_2}$  at the cathode side (b).

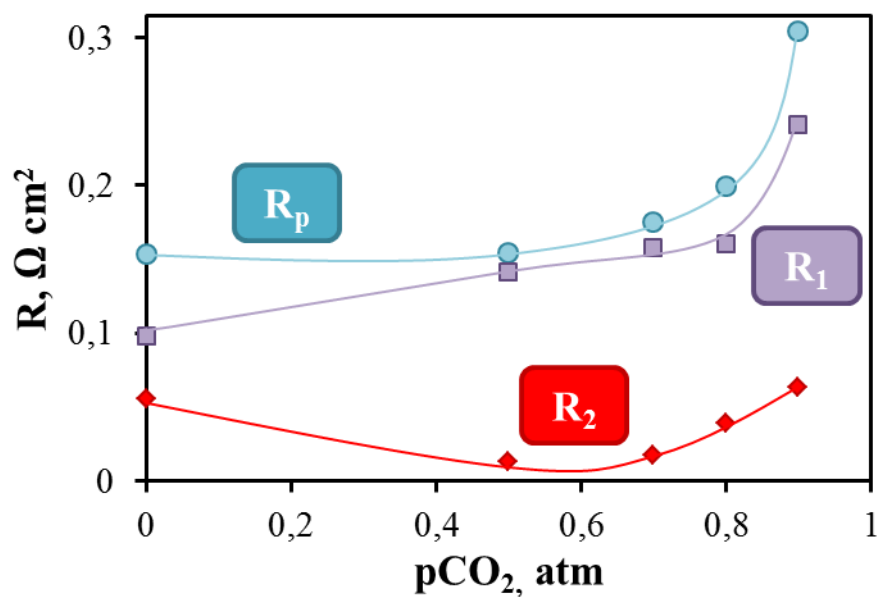


**Fig. S5** Total polarization resistances of the electrodes and its high frequency ( $R_1$ ) and medium frequency ( $R_2$ ) components as a function of  $\text{pCO}_2$  at the cathode side under the bias of 1.3 V. Lines are indicated for convenience of data perception.

## References

- [S1] [http://www.ihte.uran.ru/?page\\_id=3142](http://www.ihte.uran.ru/?page_id=3142).
- [S2] D. Medvedev, J. Lyagaeva, G. Vdovin, S. Beresnev, A. Demin, P. Tsiakaras, *Electrochim. Acta*, 2016, **210**, 681.
- [S3] E. Ivers-Tiffee, A. Weber, *J. Ceram. Soc. Jap.*, 2017, **125**, 193.
- [S4] F. He, D. Song, R. Peng, G. Meng, S. Yang, *J. Power Sources*, 2010, **195**, 3359.
- [S5] Y. Gan, J. Zhang, Y. Li, S. Li, K. Xie, J.T. S. Irvine, *J. Electrochem. Soc.*, 2012, **159**, F763.
- [S6] K. Xie, Y. Zhang, G. Men, J.T.S. Irvine, *J. Mater. Chem.*, 2011, **21**, 195.
- [S7] L. Bi, S.P. Shafi, E. Traversa, *J. Mater. Chem. A*, 2015, **3**, 5815.
- [S8] S. Yang, Y. Wen, J. Zhang, Y. Lu, X. Ye, Z. Wen, *Electrochim. Acta*, 2018, **267**, 269.
- [S9] D. Huan, N. Shi, L. Zhang, W. Tan, Y. Xie, W. Wang, C. Xia, R. Peng, Y. Lu, *ACS Appl. Mater. Interfaces*, 2018, **10**, 1761.
- [S10] S. Sun, Z. Cheng, *J. Electrochem. Soc.*, 2017, **164**, F3104.
- [S11] M. Zheng, S. Wang, Y. Yang, C. Xia, *J. Mater. Chem. A*, 2018, **6**, 2721.
- [S12] N. Shi, F. Su, D. Huan, Y. Xie, J. Lin, W. Tan, R. Peng, C. Xia, C. Chen, Y. Lu, *J. Mater. Chem. A*, 2017, **5**, 19664.